A HIGH POWER FACTOR FLUX-WEAKENING STRATEGY FOR PMSMS WITHOUT ELECTROLYTIC CAPACITORS

A Thesis

by

Seyit Yıldırım

Submitted to the
Graduate School of Sciences and Engineering
In Partial Fulfillment of the Requirements for
the Degree of

Master of Science

in the
Department of Electrical and Electronics Engineering

Özyeğin University
August 2020

Copyright © 2020 by Seyit Yıldırım

A HIGH POWER FACTOR FLUX-WEAKENING STRATEGY FOR PMSMS WITHOUT ELECTROLYTIC CAPACITORS

Approved by:

Assistant Professor Ahmet Tekin, Advisor
Department of Electrical and Electronics Engineering
Özyeğin University

Assistant Professor Göktürk Poyrazoğlu
Department of Electrical and Electronics Engineering
Özyeğin University

Professor Musa Alcı
Department of Electrical and Electronics Engineering
Ege University

Date Approved: 20 August 2020

To my family

ABSTRACT

Nowadays, large electrolytic capacitors are being replaced with small film capacitors in single phase to three phase motor drive inverters. The inverter is easy to control as the large electrolytic capacitor keeps the dc bus voltage almost constant. However, this particular electrolytic capacitor is expensive, large and it is the device with the shortest lifetime in the overall inverter system. Also, the use of electrolytic capacitors requires additional PFC circuit and pre-charging circuit. If a small film capacity is to be used instead, cost and overall size are reduced, and the product lifetime is increased significantly. However, in the case of smaller capacitors the dc-link voltage fluctuates at a rate twice of the source frequency and this in return causes control difficulties. In order to handle this issue, many methods have been proposed in the literature. This paper introduces a somehow different flux-weakening strategy to solve the mentioned problem. Also the proposed method provides power factor improvement and input current harmonic reduction in comparison to available traditional methods.

ÖZETÇE

Günümüzde, tek faz AC beslemeli üç faz motor sürücü kartlarında büyük kapasiteli elektrolitik kondansatörler yerine küçük kapasiteli film kondansatörler kullanılmaya başlanmaktadır. Büyük elektrolitik kondansatör dc bara gerilimini neredeyse sabit tuttuğundan motor kontrolü kolaydır. Ancak elektrolitik kondansatörler pahalıdır ve kart üzerinde kapladığı alan büyüktür. Ayrıca sürücü kartında en kısa kullanım ömrüne sahip olan malzemedir. Bununla birlikte elektrolitik kondansatörlerin kullanımı ek PFC devresi ve ön şarj devresi gerektirir. Bunun yerine küçük bir film kapasitesi kullanılırsa maliyet ciddi derecede azalır. Kartın boyutu küçülür ve ürün ömrü önemli ölçüde artar. Bununla birlikte, film kondansatör kullanılması durumunda, dc bara gerilimi kaynak frekansının iki katı oranında dalgalanır ve bu durum motor kontrolünü zorlaştırır. Bu sorunu çözmek için literatürde birçok yöntem önerilmiştir. Bu makale, söz konusu sorunu çözmek için farklı bir akı zayıflatma stratejisi önermektedir. Ayrıca önerilen yöntem, mevcut geleneksel yöntemlere kıyasla güç faktörü iyileştirmesi ve giriş akımı harmonik performansını iyileştirir.

ACKNOWLEDGEMENTS

I would like to thank my advisor Asst. Prof. Ahmet TEKİN for his patient guidance and support. I am also grateful to all my managers, especially Raşit GÖKALAN, who did not withhold his help and support during the works. Also, I would like to thank my company Vestel for all the conveniences they provide in the use of laboratories and their valuable support during the test and characterizations.

TABLE OF CONTENTS

YÖK watermark

LIST OF TABLES

LIST OF FIGURES

LIST OF SYMBOLS

V_a, V_b, V_c	Phase A, B, C voltage
V_α,V_β	alpha, beta voltage in stationary frame
V_d, V_q	d, q axis voltage in rotating frame
i_a, i_b, i_c	Phase A B C current
i_α,i_β	alpha, beta current in stationary frame
i_d, i_q	d, q axis current in rotating frame
i_{d_ref}, i_{q_ref}	reference d, q axis current in rotating frame
i_{dr_mod}, i_{qr_mod}	modulated reference d, q axis current in rotating frame
i_{d_m}, i_{q_m}	measured d, q axis current in rotating frame
R	Stator resistance
L	Stator inductance
L_d, L_q	d, q axis inductance
λ_a, λ_b, λ_c	Stator A, B, C phases interlinkage flux
ϕ	Maximum flux linkage due to permanent magnet
ϕ_a	flux linkage due to permanent magnet
θ	Rotor electrical angle from phase A
ω	Angular speed
P_{in}	Input power
P_c	Power on dc link capacitor
P_{inv}	Inverter power
ϑ	AC grid angle
V_{in}	Maximum grid voltage
I_{in}	Maximum grid current

CHAPTER I

INTRODUCTION

Electric motors are used in most of the products in our house, industrial applications, transportation vehicles, military applications, briefly in all areas of our lives. The vast majority of electricity consumption in the world belongs to motors. Given the scarce energy resources and rising energy costs in the world, it is essential to use electric motors as efficiently as possible. The use of high efficiency electric motors in developed countries has become mandatory in most applications. Therefore, high efficiency motor design and efficient driving of these motors are increasingly important. Especially in white goods applications, induction and brushed dc motors are replaced by permanent magnet synchronous motors (PMSM). PMSM is more efficient than induction and brushed dc motors, as well as its silent operation and lack of maintenance, provides an extra advantage in white goods applications. Besides these features, driving a PMSM is not simple as other motors. It requires an inverter board and complex control system.

For PMSM drive, conventional single phase to three phase inverter block diagram is shown Figure 1.0.1. Large electrolytic capacitors are used to keep dc-link voltage flat for high quality supply and hence better motor performance. If dc-link voltage is almost constant, traditional control techniques will be introduced in Chapter III can be applied.

Using a large electrolytic capacitor poses some challenges, most notably its much shorter lifetime. Hence, this huge input capacitor in most cases determines the overall lifespan of the inverter board. Also, it can't be ignored that this large dc-link

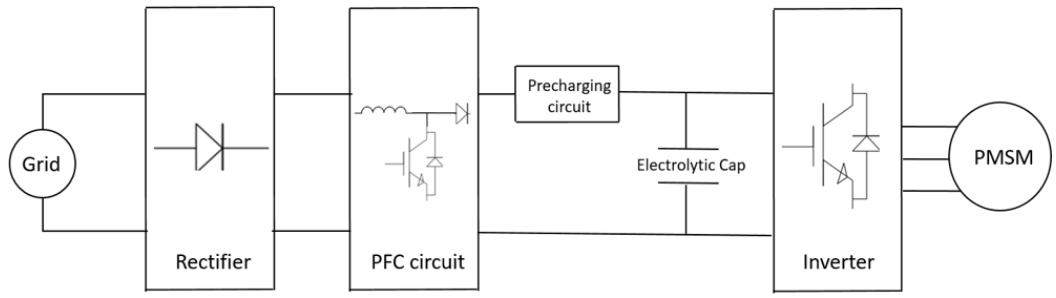

Figure 1.0.1: Conventional single phase to three phase inverter.

electrolytic capacitor has a quite reputable weakness in reliability [1]. Other important issues about electrolytic capacitor can be cited as its large volume and high cost. Moreover, large electrolytic capacitors cause low input power factor and high inrush current. Especially in industrial applications and home appliances such as white goods, these problems very critical for safety, reliability and EMC requirement.

In conventional method shown in Figure 1.0.1, active or passive PFC circuit is used to solve low input power factor problem due to large input capacitor. Also a pre-charging circuit is used to overcome high inrush current issue. This extra circuit relating to electrolytic capacitor has also high cost and takes up big space. In addition to the poor reliability of the electrolytic capacitor itself, the extra circuits that need to be added due to the capacitor reduce the overall reliability of the system. If the motor control can be achieved with the inverter board designed by using a small film capacitor instead of a large electrolytic capacitor, the mentioned negativities caused by the large electrolytic capacitor itself and the extra circuits required for its use will be solved. In case of using a small film capacitor, the last block diagram of the system will be as in Figure 1.0.2. As seen in the figure, the system is quite simplified. In this case, the cost of the system decreases considerably, the size of the inverter board decreases and the reliability of the system increases. All these mentioned improvements are a great source of motivation for industrial applications.

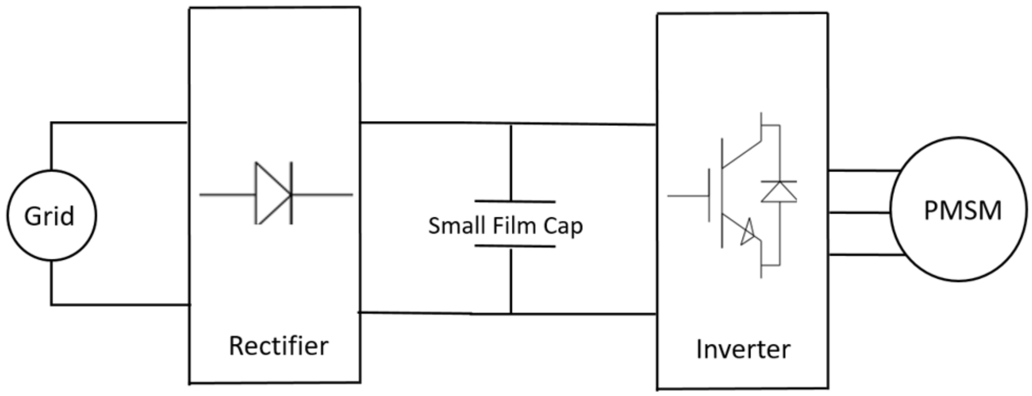

Figure 1.0.2: Electrolytic capacitorless single phase to three phase inverter.

Besides all these, using a small film capacitor brings various control difficulties. If small film capacitor is used in single phase system, the rectified dc-link voltage fluctuates at twice frequency of the ac source voltage source frequency [2]. As the output power increases, the dc link voltage waveform will be similar to the rectified ac signal waveform. Fluctuating Dc-link voltage causes torque fluctuations and a speed control difficulties. In order to overcome these problems various correction techniques are proposed in literature. Many researches overcome this problem by modifying the d-axis and q-axis current references of the inverter because conventional field-oriented vector control is not sufficient to speed control of PMSM driven by inverter with a small film capacitor.

The main objective of this thesis is to provide speed control of the permanent magnet synchronous motor by an inverter board designed with a small film capacitor. Chapter II gives information about permanent magnet synchronous motors. Chapter III introduces the basic control types of PMSM with electrolytic capacitor and Chapter IV reviews previous works for speed control of PMSM without electrolytic capacitor. Chapter IV introduces the proposed method for speed control of PMSM without electrolytic capacitor.

CHAPTER II

PERMANENT MAGNET SYNCHRONOUS MOTORS

A synchronous machine is an ac machine whose speed under steady-state conditions is proportional to the frequency of the current in its armature. The rotor, along with the magnetic field created by the dc field current on the rotor, rotates at the same speed as the rotating magnetic field produced by the armature currents, and a steady torque results [3]. The classification of AC synchronous machines are shown in Figure 2.0.1.

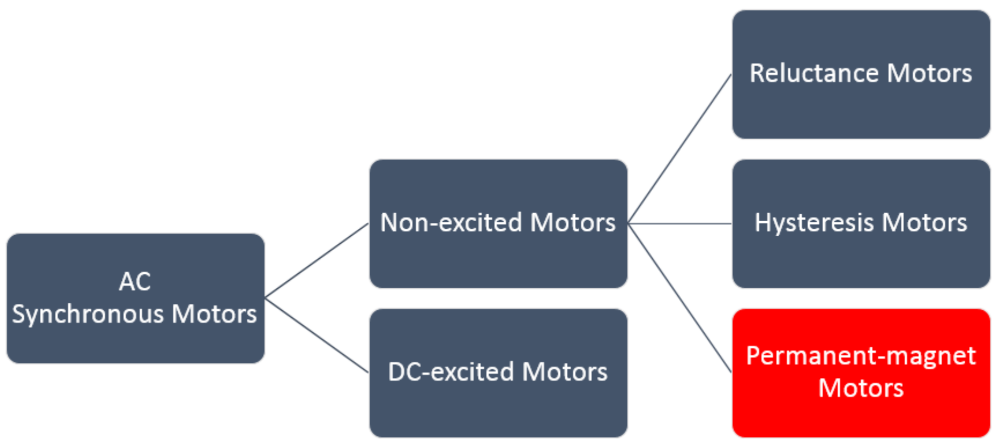

Figure 2.0.1: The classification of AC synchronous machines

Unlike non-excited synchronous motors in DC excited synchronous motors, the rotor also has windings. Therefore, it requires direct current (DC) supply to create a magnetic field in the rotor. Supplying the rotor with direct current requires an extra mechanical structure such as slip rings compared to non-excited synchronous motors.

A permanent-magnet synchronous motor (PMSM) is a non-excited synchronous motor. In this motor type, permanent magnets are used to create a magnetic field on the rotor. As magnets with higher flux density such as neodymium magnets develop over the years, permanent magnet synchronous motors have become popular.

Since there are no mechanical parts such as brushes or slip rings in permanent magnet synchronous motors, they work very quietly. Especially in applications where sound is very important, such as white goods, the permanent magnet synchronous motor stands out with its silent operation feature.

2.1 Classification of PMSM's

Permanent magnet synchronous motors, like all electric motors, consist of rotors and stators. However, it can be designed with many different rotor and stator structures. PMSM's can be classified as concentrated windings and sinusoidally distributed windings according to stator winding types. When the stator windings are concentrated, the back emf waveform is trapezoidal and it is called as brushless dc (BLDC) machine. When the stator windings are sinusoidally distributed, the back emf waveform is sinusoidal and it is called as permanent magnet ac (PMAC) machine. The mentioned winding types are shown in Figure 2.1.1.

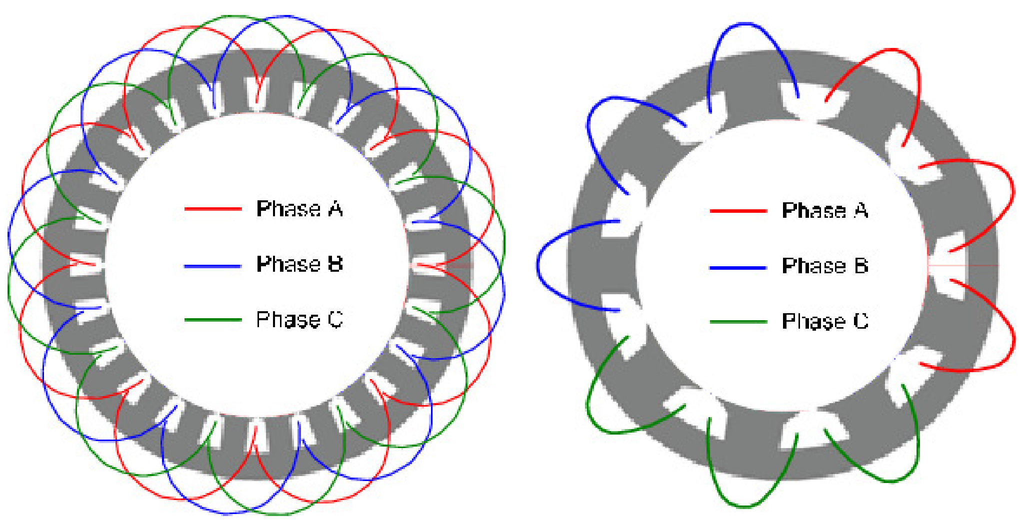

Figure 2.1.1: The classification of PMSM's according to stator winding types (left one is distributed winding and right one is concentrated windings). [4]

PMSMs are also classified according to rotor configuration as inner or interior rotor and outer or exterior rotor which is illustrated in Figure 2.1.2. PMSM that has an inner rotor achieve same speed and torque at a lower weight and smaller size than the PMSM which has an outer rotor. Therefore, PMSMs which has inner rotor come to the fore in applications where space and weight are the design constraint [5]. In inner rotor PMSMs has also cooling advantage since the stator windings are placed outer frame. On the other hand, outer rotor type PMSM has higher inertia compared to inner type PMSM due to big rotor diameter. Higher inertia provides more precise speed control.

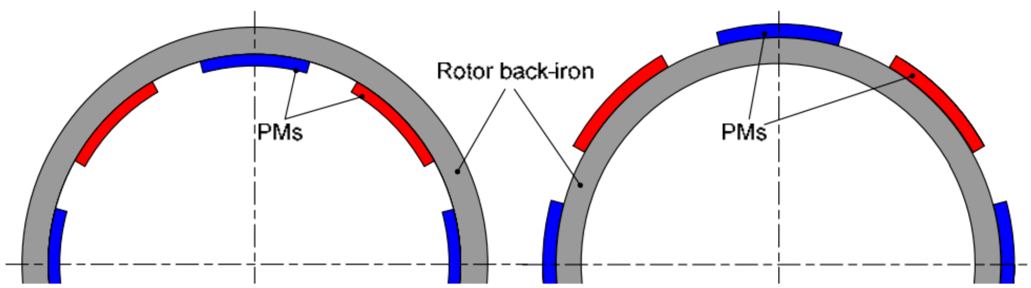

Figure 2.1.2: The classification of PMSM's according to rotor position (left one is outer rotor and right one is inner rotor). [4]

PMSMs can be separated according to magnets placement on rotor as interior permanent magnet motors (IPM) and surface mounted permanent magnet motors (SPM) which is indicated in Figure 2.1.3. Surface mounted rotor type (SPM) has more mechanical weakness compared to interior permanent magnet rotor type (IPM) due to magnets position. Therefore, IPM type rotor will be safer than SPM type rotor in high speed applications. On the other hand, IPM type rotor is capable of producing reluctance torque that is not in SPM type rotor. Thus, in the IPM type rotor with less magnet, equal torque can be produced compared to SPM type rotor.

PMSM's are also classified according to direction of the field flux as radial flux and axial flux motors which is illustrated in Figure 2.1.4. Direction of the field flux is

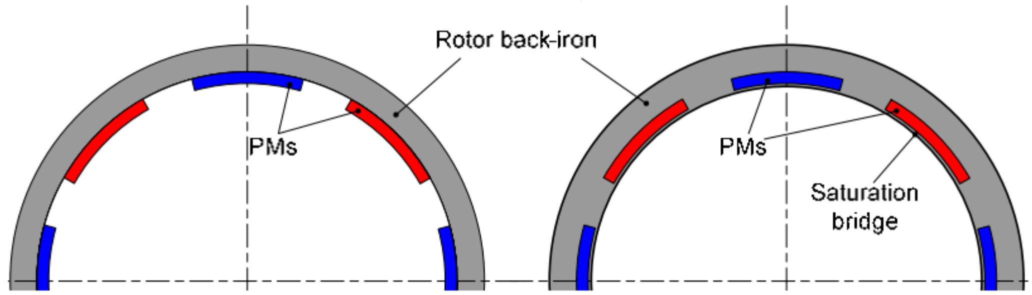

Figure 2.1.3: The classification of PMSM's according to magnet placement (left one is SPM and right one is IPM). [4]

in parallel with the axis of the shaft in axial flux motors. On the contrary, in radial flux machine, direction of the field flux is perpendicular to the axis of the shaft. One of the most decisive difference between radial flux and axial flux is axial motors have higher torque density compared to axial flux at the same volume.

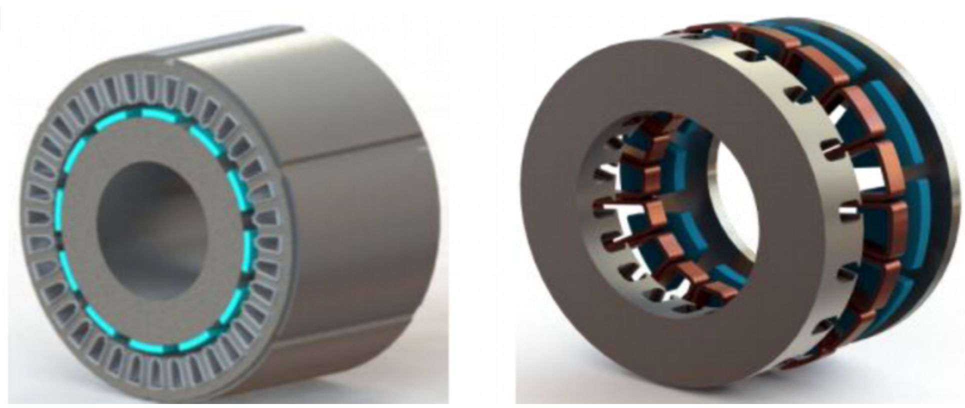

Figure 2.1.4: The classification of PMSMs according to direction of the field flux (left one is radial flux and right one is axial flux). [6]

As mentioned above, PMSMs can be designed in many different mechanical structures. The most appropriate design should be used according to the requirements of the application.

2.2 *Mathematical Model of PMSMs*

Mathematical modeling of a circuit, a device or a machine to be controlled is very important. In this way, necessary analyzes can be made and the most appropriate control technique can be developed. Conceptual diagram of balanced three phase PMSM is illustrated in Figure 2.2.1 with neglecting mutual inductance. Three phase voltage equations are as follows.

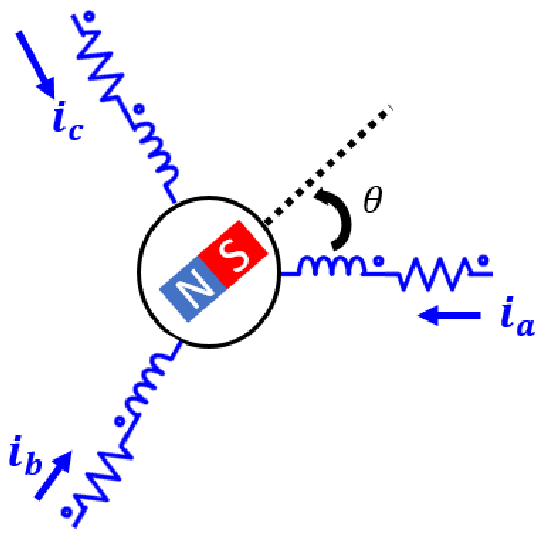

Figure 2.2.1: Conceptual diagram of balanced three phase PMSM.

$$V_a = R \cdot i_a + \frac{d\lambda_a}{dt} \tag{2.2.1}$$

$$V_b = R \cdot i_b + \frac{d\lambda_b}{dt} \tag{2.2.2}$$

$$V_c = R \cdot i_c + \frac{d\lambda_c}{dt} \tag{2.2.3}$$

where

$$\lambda_a = L \cdot \frac{di_a}{dt} + \phi \cdot cos(\theta) \tag{2.2.4}$$

$$\lambda_b = L \cdot \frac{di_b}{dt} + \phi \cdot cos(\theta - \frac{2\pi}{3}) \tag{2.2.5}$$

$$\lambda_c = L \cdot \frac{di_c}{dt} + \phi \cdot cos(\theta + \frac{2\pi}{3}) \tag{2.2.6}$$

i_a , i_b and i_c are vectoral phase current components. So they can be represented with phasor or vector diagram. Three phase balanced phase currents and their phasor diagram on motor are illustrated in like in Figure 2.2.2

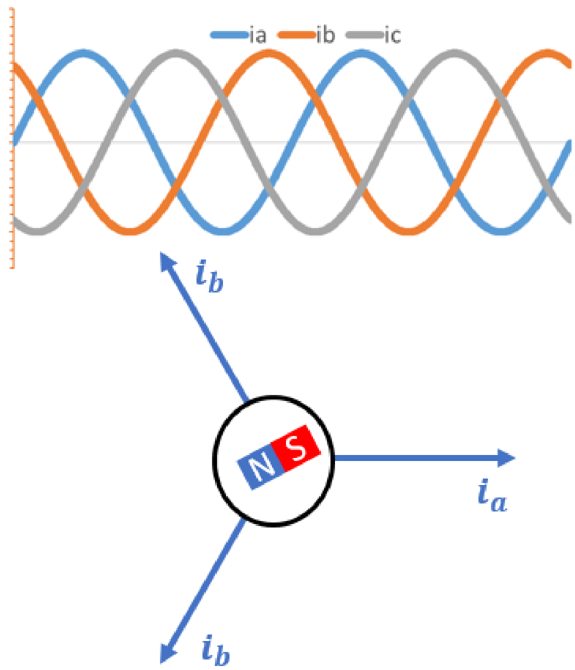

Figure 2.2.2: Balanced three phase reference frame

In the case of complex motors such as PMSM, the equations of the motor are quite complex for a control algorithm. Therefore, when modeling such engines, it is generally benefited from mathematical transformations. Thus, simpler equations emerge and stable control systems are designed.

Clarke and Park transformations are used in vector control applications. Thanks to these transformations, the control process becomes easier. Clarke transformation provides the transition from a 3-phase system to a 2-phase system (stationary frame) that is perpendicular to each other. Then Park transform provide the transition from a 2-phase system (stationary frame) to a rotating frame system.

2.3 Stationary Reference Frame

By helping Clarke transformation, i_a, i_b and i_c components are transformed to orthogonal two axis components as i_α and i_β. In Figure 2.3.1, orthogonal i_α and i_β waveform and their phasor diagram on motor are represented. This α, β frame is called stationary reference frame. This transform can be done by following equations.

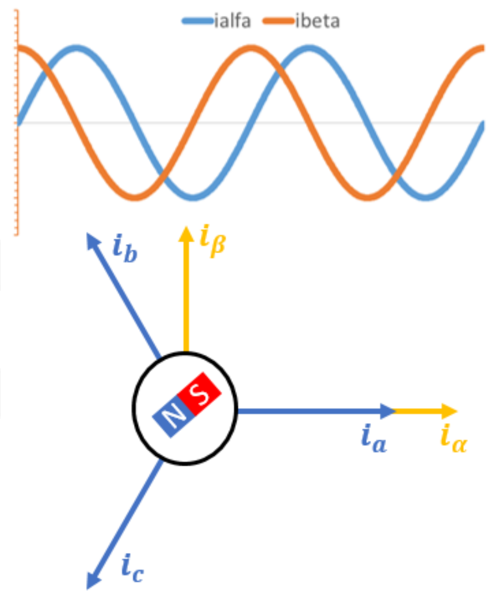

Figure 2.3.1: Two phase or stationary reference frame

$$i_\alpha = \frac{2}{3} \cdot i_a - \frac{1}{3} \cdot (i_b - i_c) \tag{2.3.1}$$

$$i_\beta = \frac{2}{\sqrt{3}} \cdot (i_b - i_c) \tag{2.3.2}$$

If the system is balance three phase system, then;

$$i_a + i_b + i_c = 0 \tag{2.3.3}$$

Under this condition, Clarke transform can be rewritten as follows

$$i_\alpha = i_a \tag{2.3.4}$$

$$i_\beta = \frac{1}{\sqrt{3}} \cdot (i_a + 2 \cdot i_b) \tag{2.3.5}$$

2.4 Rotating Reference Frame

By helping Park transformation, i_α and i_β components are transformed to o i_d and i_q. In Figure 2.3.1, i_d and i_q waveform and their phasor diagram on motor are represented. This i_d and i_q frame is called rotating reference frame. This transform can be done by following equations.

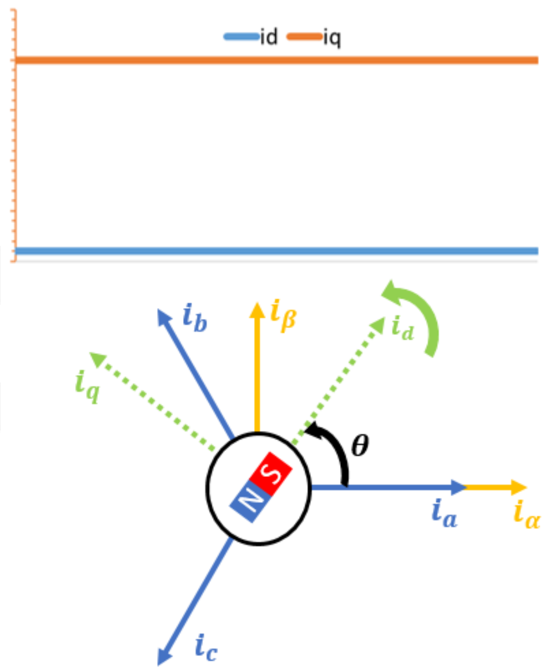

Figure 2.4.1: Rotating reference frame

$$i_d = i_\alpha \cdot cos(\theta) + i_\beta \cdot sin(\theta) \tag{2.4.1}$$

$$i_q = i_\beta \cdot cos(\theta) - i_\alpha \cdot sin(\theta) \tag{2.4.2}$$

When Clarke and Park transforms are applied to three phase voltage equations, voltage equations are rewritten in rotating frame as follows.

$$V_d = i_d \cdot R + L_d \cdot \frac{di_d}{dt} - i_q \cdot \omega \cdot L_q \tag{2.4.3}$$

$$V_q = i_q \cdot R + L_q \cdot \frac{di_q}{dt} + i_d \cdot \omega \cdot L_d + \omega \cdot \phi_a \tag{2.4.4}$$

where

$$\phi_a = \sqrt{\frac{3}{2}} \cdot \phi \tag{2.4.5}$$

Current and voltage signals in the stationary reference frame have a sinusoidal waveform, while in the rotating reference frame currents and voltage signals have a dc waveform due to d and q axis rotating synchronously with the rotor.

Speed and current controllers with dc waveforms are designed simpler and can be applied easily. That's why Clarke and Park transformations are very useful and important in controlling 3-phase systems and are used by everyone.

CHAPTER III

TRADITIONAL CONTROL METHODS OF PMSM WITH LARGE ELECTROLYTIC CAPACITOR

In this chapter, traditional control methods of PMSM driven by an inverter with electrolytic capacitor. Depending on the requirement of the application different control techniques are used in the industry for PMSM control. PMSM control techniques can be classified in Figure 3.0.1

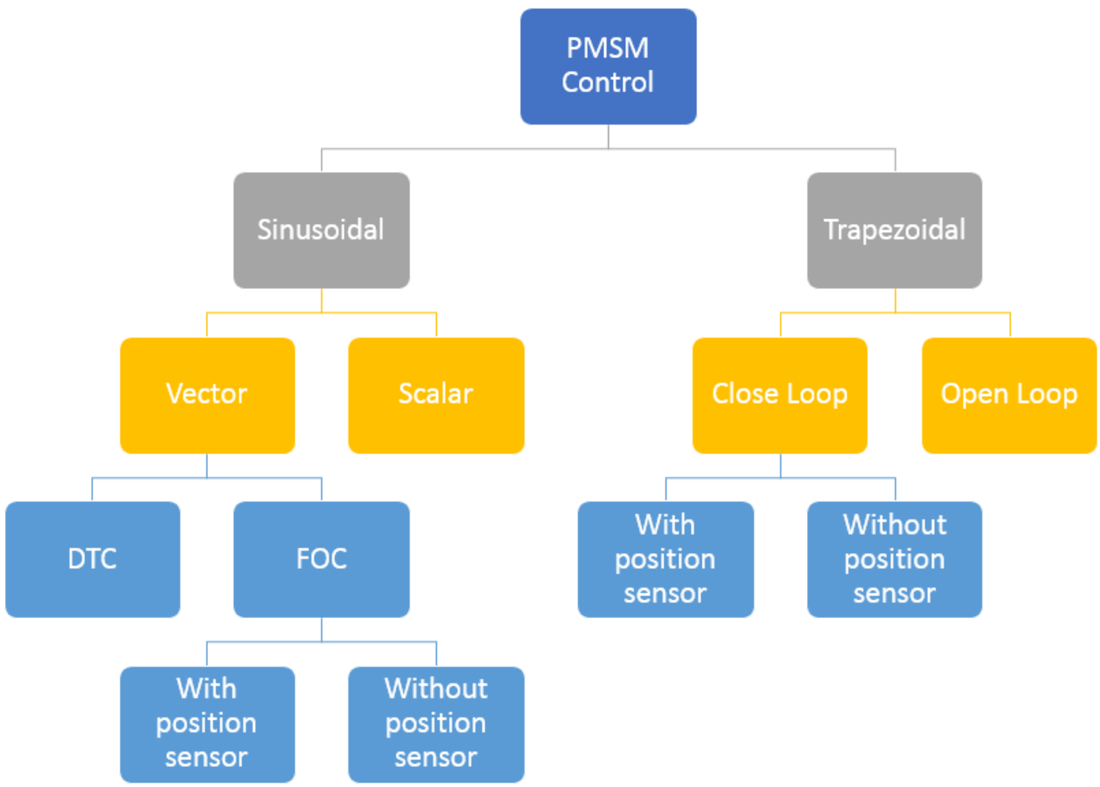

Figure 3.0.1: The classification of PMSM control techniques

3.1 Trapezoidal Control

Trapezoidal control technique which is also called six step control one of the simplest control technique of a permanent magnet synchronous motor. Trapezoidal control technique is more appropriate for PMSM which has trapezoidal back emf. However, it can be used for PMSM which has sinusoidal back emf. However, in this use, performance loss will occur such as decreasing average torque value and increasing torque ripple value.

In trapezoidal control, the switching loss is lower compared to sinusoidal control since the IGBTs in the inverter is switched only 6 times in an electrical period. This is one of the major advantages of the trapezoidal control technique.

3.1.1 Open Loop

Implementing open loop trapezoidal control technique is quite simple as seen in the Figure 3.1.1. Therefore, it can be used simply with low performance microcontrollers. However, this method has considerable disadvantages.

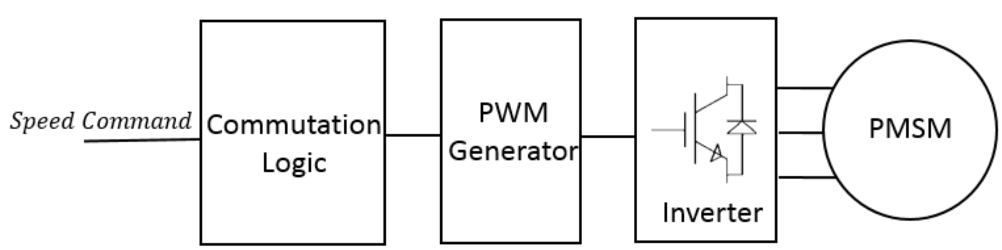

Figure 3.1.1: Open loop trapezoidal control

PMSM can easily be out of synchronism because there is no feedback loop in the open loop trapezoidal control. It is not efficient drive technique due to lack of rotor position information. Even if synchronization is not lost, heat loss will be high as there is no efficient driving. Therefore, it is not preferred in industrial applications.

3.1.2 Close Loop

Close loop trapezoidal control provide more stable control since there is a feedback loop. But, if load torque is changing very quickly, loss of motor control occurs because the control loop operates only 6 times. Besides, if load torque does not change very quickly such as in pump or fan applications, this method provide very stable motor control. Close loop trapezoidal control can be divided into two groups according to position sensor usage.

3.1.2.1 Close Loop with Position Sensor

Hall effect sensor is used as position sensor in close loop trapezoidal control. In three phase system, three hall sensors are built into motors. Block diagram of close loop trapezoidal control with position sensor is shown Figure 3.1.2.

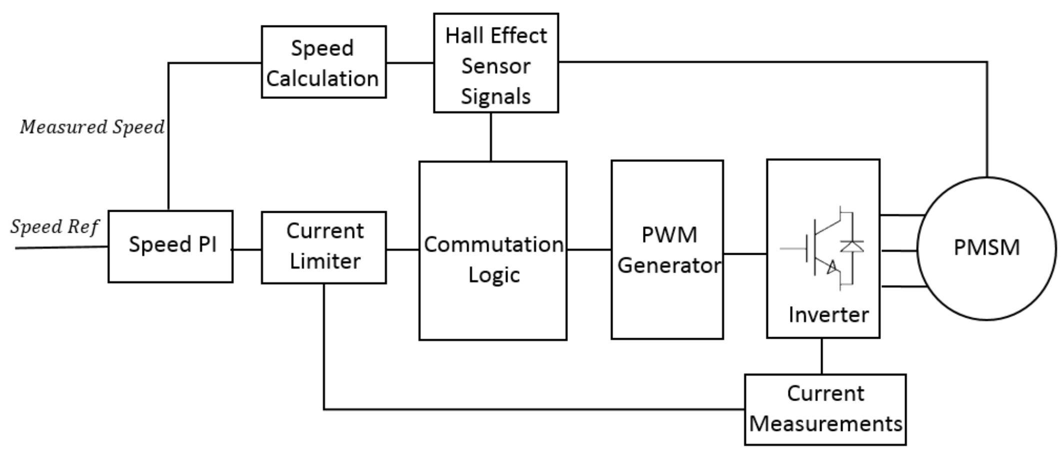

Figure 3.1.2: Close loop trapezoidal control with position sensor

The installation cost of the hall effect sensor is the disadvantage of this system. To get rid of this cost, position information is detected by back emf estimator using inverter output voltages.

3.1.2.2 *Close Loop without Position Sensor*

In this system position information is calculated from back emf voltages. Therefore, this system requires a more complex control. However, this system is advantageous in terms of cost since there is no need for any position sensor. Block diagram of close loop trapezoidal control without position sensor is shown Figure 3.1.3.

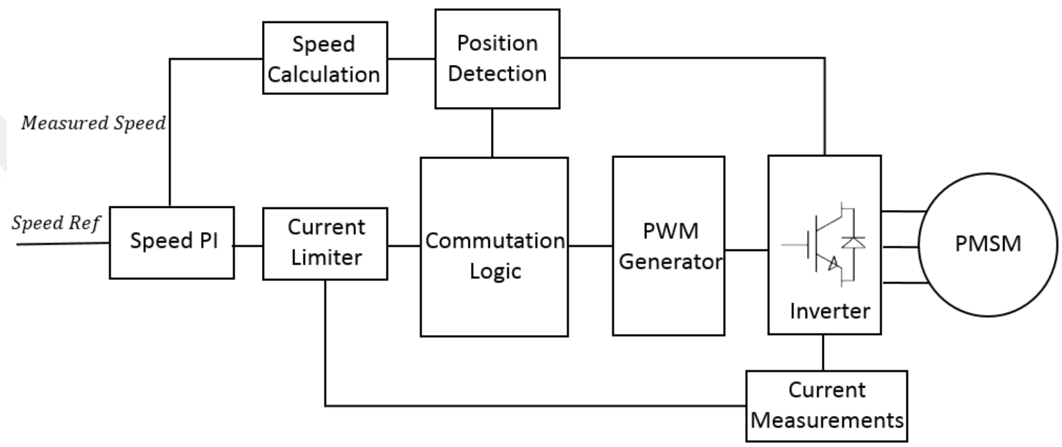

Figure 3.1.3: Close loop trapezoidal control without position sensor

3.2 *Sinusoidal Control*

Sinusoidal control technique is more appropriate for PMSM which has sinusoidal back emf. In this technique, the switching loss is higher compared to trapezoidal control since the IGBTs in the inverter is switched every switching period. Sinusoidal control is also divided into two groups as scalar control and vector control.

3.2.1 Scalar Control

The principle of the scalar control is to maintain a constant V/Hz ratio almost through the whole speed range operation since only the magnitude and frequency of the supply voltages is controlled. [7]. Block diagram of scalar control is shown Figure 3.2.1.

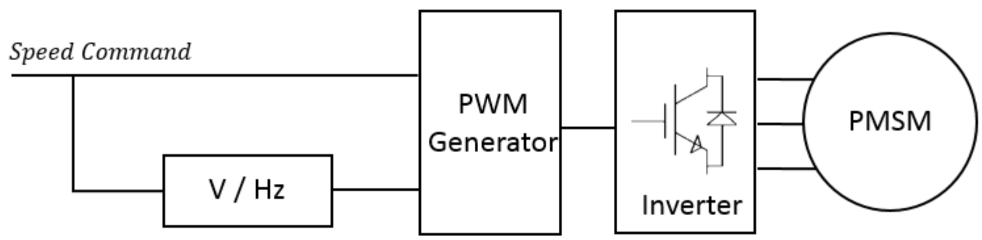

Figure 3.2.1: Scalar control method

Scalar motor control technique has no good dynamic performance at variable load conditions because the stator currents are not directly controlled and torque is not controllable. Because of that, PMSM can be out of synchronism and loss of control occur very easily. So, The scalar control technique is not proper for the control of PMSM at requiring high dynamics applications.

When high dynamics performance over wide speed range is desired, vector control technique is optimal control technique.

3.3 Vector Control

Vector control provides higher performance compared to scalar control. Almost all the disadvantages of scalar control mentioned in previous section are eliminated by vector control technique. The main idea of vector control is to control not only the magnitude and frequency of the supply voltages but also the angle.[7]

In scalar control torque and flux component are coupled. This inherent coupling make the system prone to instability [8]. On the other hand, the vector control allows separate closed loop control of both the flux and torque component, hence, achieving a similar control structure to that of a separately excited DC machine which is very simple to control.[9]

Vector control techniques can be divided into two main groups as direct torque control (DTC) and field oriented control (FOC).

3.3.1 Direct torque control (DTC)

Implementation of direct torque control (DTC) technique is simpler compared to field oriented control (FOC) that will be introduced in the next section. General block diagram of direct torque control is shown Figure 3.3.1.

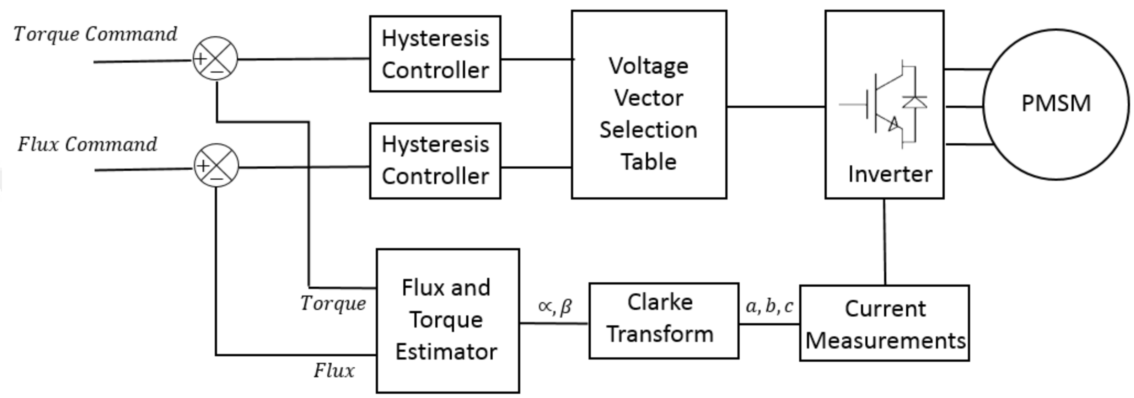

Figure 3.3.1: Direct Torque Control of PMSM

As seen in Figure 3.3.1, in direct torque control, all calculations are done in stationary reference frame. Since there is no need for Park transform that requires rotor position information, position sensor requirement is eliminated. The control system become easier since there is no need any position sensor and Park transform which is relatively complex. Although the DTC application has a simple control technique, its dynamic response is quite high. In addition, the DTC technique is not too dependent on motor parameters as in the FOC technique. DTC tecnique require only stator resistance information as motor parameters [8].

One of the major disadvantages of DTC technique is that it has high torque and current ripples during steady state operation. [7].

3.3.2 Field-oriented control (FOC)

Unlike the DTC, in direct torque control speed and current controllers operate in rotating reference frame which requires rotor position information. Because of that FOC includes more complex mathematical process. So it requires higher performance microcontroller.

If the dynamic responses of DTC and FOC are compared, it can be said that both methods provide a good performance with quicker torque dynamics in case of DTC. In addition to this, FOC has good steady state characteristics compared to DTC. [10]

As mentioned before, FOC technique require rotor position information. According to whether the sensor is used for rotor position information or not, we can examine the FOC technique in two separate groups.

3.3.2.1 FOC with position sensor

General block diagram of field oriented control with position sensor is shown in Figure 3.3.2. Generally, incremental encoder is used as a position sensor. Since speed is the derivative of the position, no separate sensor is required for speed information.

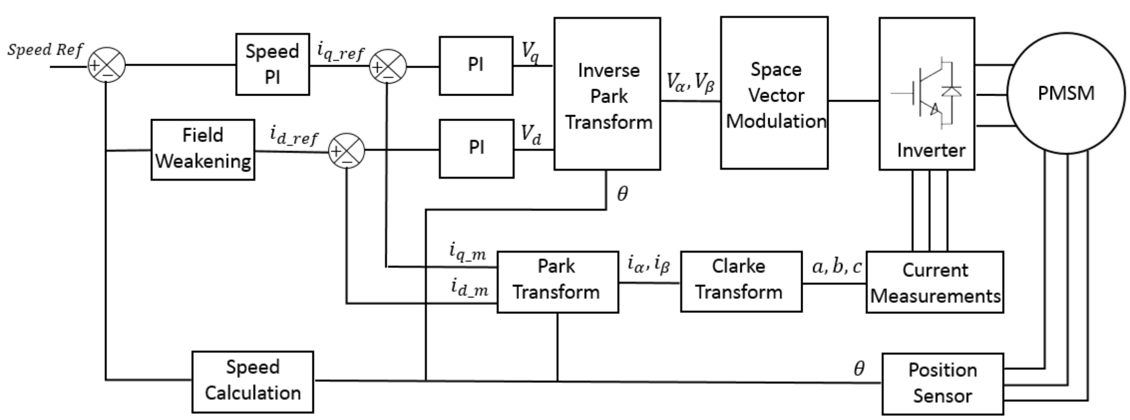

Figure 3.3.2: General field oriented control diagram with position sensor

3.3.2.2 FOC without position sensor

General block diagram of field oriented control without position sensor is shown in Figure 3.3.2.

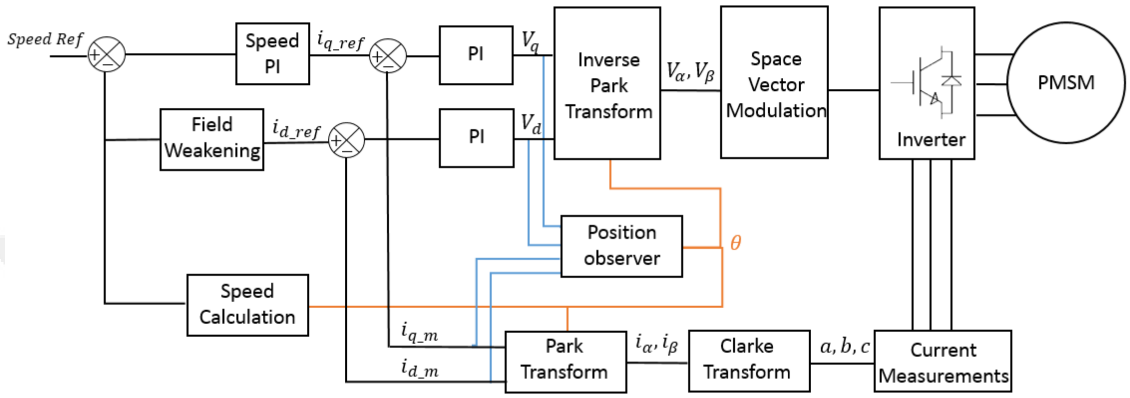

Figure 3.3.3: General field oriented control diagram without position sensor

To obtain rotor position and speed information, many different types of observers are used in industrial applications and academic works. The stability of the system directly depends on the stability of the observer used for the rotor position. Since these observer contains complex mathematical operations, a higher performance processor will be needed in this technique compared to other techniques. Sliding mode observer and Luenberger observer are commonly used as rotor position estimator.

Overall block diagram of sensorless field oriented control of PMSM with power circuit is shown in Figure 3.3.4. In the figure, electrolytic capacitor is used to keep dc-link voltage almost constant for high quality supply and hence better motor performance. In typical white goods applications, electrolytic capacitor value is around 300-1500uF. In this thesis study, a new stable and efficient motor control algorithm is proposed when 5-15uF film capacitor is used instead of higher value electrolytic capacitor.

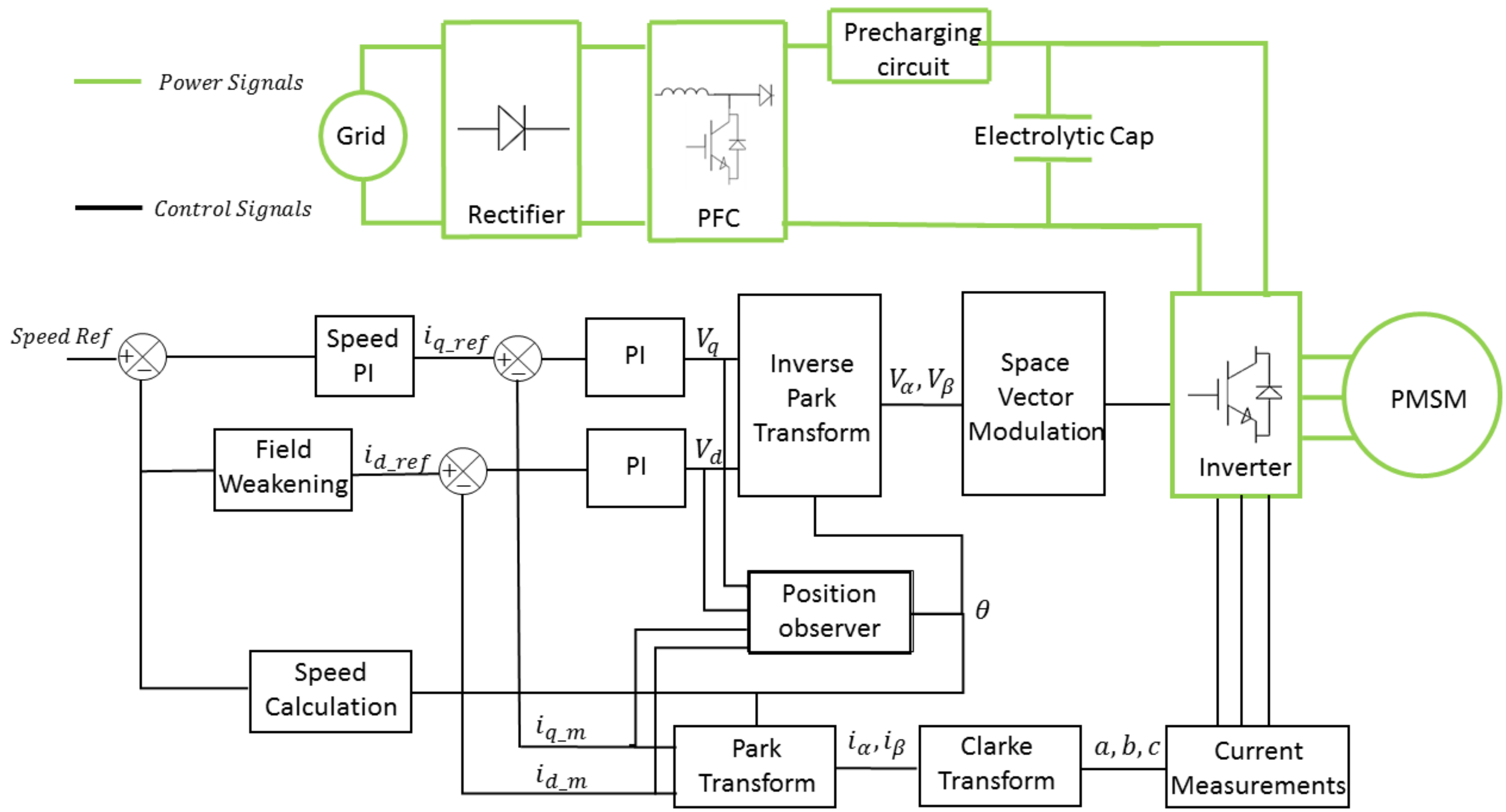

Figure 3.3.4: Overall field oriented control diagram without position sensor

CHAPTER IV

PREVIOUS WORKS FOR SPEED CONTROL OF PMSM WITHOUT ELECTROLYTIC CAPACITOR

Generally, motor drive systems that do not use electrolytic capacitors are briefly named as "capacitorless" in the literature. Therefore, the term "capacitorless" will be used more in the next sections.

As mentioned in introduction chapter, For PMSM drive, in conventional single phase to three phase inverter which is shown before in Figure 1.0.1 large electrolytic capacitors are used to keep dc-link voltage flat for high quality supply and hence better motor performance. If dc-link voltage is almost constant, traditional control techniques previously introduced in chapter III can be applied.

Although using a large electrolytic capacitor is useful for dc bus supply, it brings many problems to be solved. One of the major disadvantages of using large electrolytic capacitor is it has short life time and quite reputable weakness in reliability. [1]. Since the electrolytic capacitor has the shortest lifetime in the drive system, the lifetime of the overall drive system is directly related to the electrolytic capacitor.

Another disadvantages of using a large electrolytic capacitor is that it requires pre-charging circuit to avoid high inrush current. Inrush current value can be calculated from capacitor current equation below.

$$i_c = C \cdot \frac{dv_c}{dt} \tag{4.0.1}$$

At the first energization, the term of $\frac{dv_c}{dt}$ will be too high since capacitor voltage is zero before energization. Also amplitude of inrush current is proportional with capacitor value. In typical white goods applications, electrolytic capacitor value is around 300-1500uF. As a result, these high inrush currents caused by electrolytic capacitors should be avoided. In generally, two types of inrush current limiter circuits which is also called pre-charging circuits are used. This two types are passive inrush current limiter and bypass circuit. Passive inrush current limiter is very simple. It suggests to adding resistance in series with capacitor. This resistance can be normal resistance or thermistors. However, since this resistance is constantly active throughout the operation, it will consume unnecessary power and increase the heat on the board. On the other hand, bypass circuit consists of a resistor in series with capacitor and relay or switch such as Mosfet. In the bypass system, resistor is only active at first energization. After that, resistor is bypassing by helping a relay or switch. In this way, there will be no continuous power consumption. As a result, pre-charging circuits has extra cost and it takes up space on the board. Also according to pre-charging circuit type, it can cause extra power consumption.

Another major disadvantages of using large electrolytic capacitor as dc-link is that it causes low input power factor. Therefore, active or passive a power factor correction (PFC) circuit is required to solve low input power factor problem. This PFC circuits has high cost and take up big space.

In order to overcome all these problems mentioned before section, many different techniques have been proposed. Studies in the literature can be divided into two main groups depending on whether or not any capacitor is used. The first is the matrix converter topology shown in Figure 4.0.1, which does not contain a dc link capacitor [11].

However, since this method contains a large number of switches, it is both very difficult to control and unfavorable in terms of space and cost . Also this topology can not use single phase ac source.

Other method is using several micro farad film capacitor instead of several hundred micro farad electrolytic capacitor as dc link capacitor.[2, 12, 13, 14, 15, 16, 17] Block diagram of this system was shown in Figure 1.0.2 in introduction chapter. In this

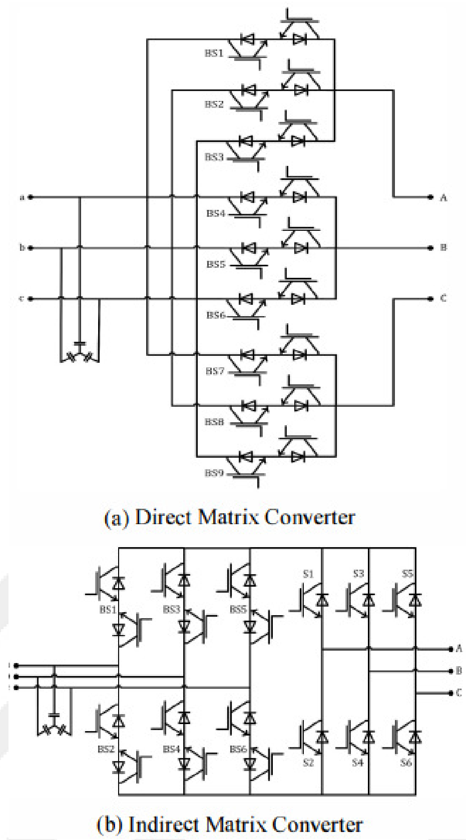

Figure 4.0.1: Matrix Converter [11]

system, since the PFC circuit and the pre-charging circuit are not needed, the system volume is significantly reduced, and cost is also reduced. Moreover, due to switchover to a film capacitor, reliability weakness is also eliminated. This small film capacitor method can be utilized into two groups as single phase and three phase AC supply. There are fewer studies in the literature about single phase systems compared to three phase system. Due to scope of this thesis is single phase ac source system such as white goods applications, single phase ac source system will be examined.

If small film capacitor is used in single phase system, the rectified dc-link voltage fluctuates at twice frequency of the ac source voltage source frequency[2]. Similar waveforms of grid voltage and dc link voltage with a small film capacitor are shown in Figure 4.0.2.

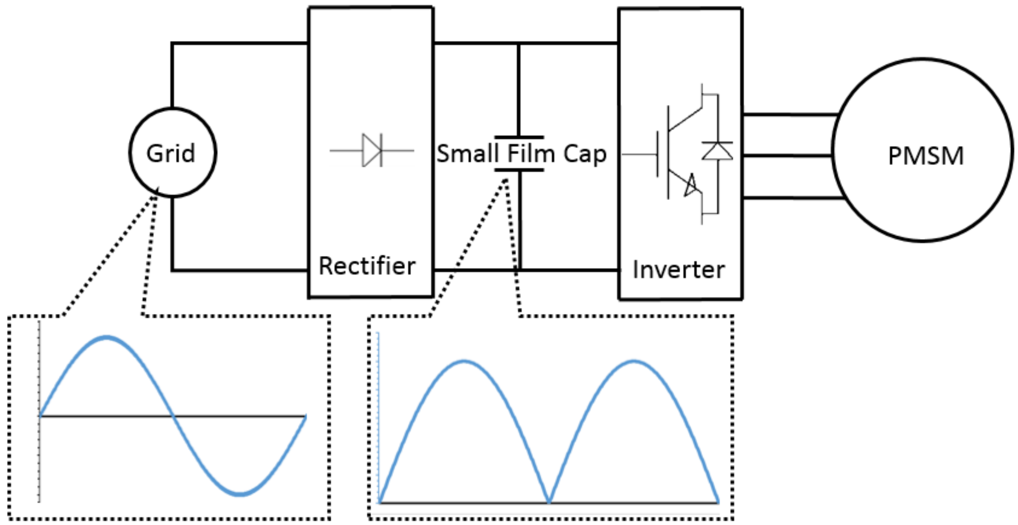

Figure 4.0.2: Grid and dc link voltages with a small film capacitor

As the output power increases, the dc link voltage waveform will be similar to the rectified ac signal waveform. In other words, as the output power increases the ratio of $Vdclink_{min}/Vdclink_{max}$ which is indicated in Figure 4.0.3 converges to zero. Also, the lower the film capacity value, the $Vdclink_{min}$ voltage level will approach zero.

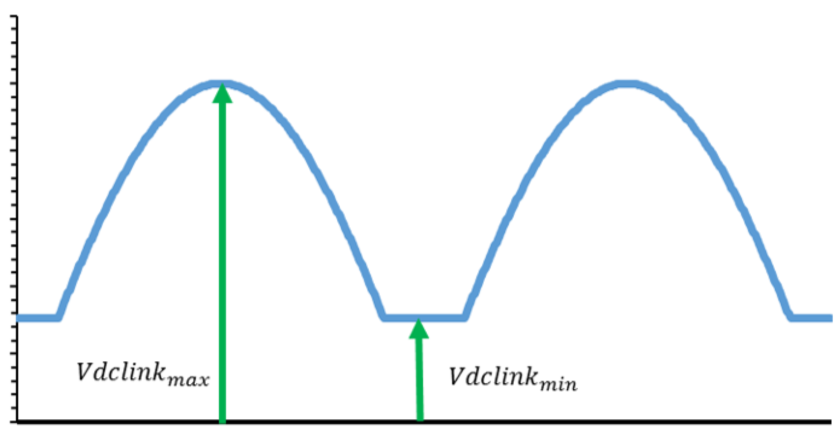

Figure 4.0.3: Dc link voltage waveform variation

$Vdclink_{min}$ voltage level decreases as the output power increases. At the same time $Vdclink_{min}$ voltage level is directly related to when rectifier diodes are conducting.

So it effects directly to input power factor. Input current waveform and dc link voltage are indicated in Figure 4.0.4. All in all, it can be said that, as the output power increases $Vdclink_{min}$ value decreases, as $Vdclink_{min}$ value decreases $t_{conduct}$ time increases which means input power factor increases.

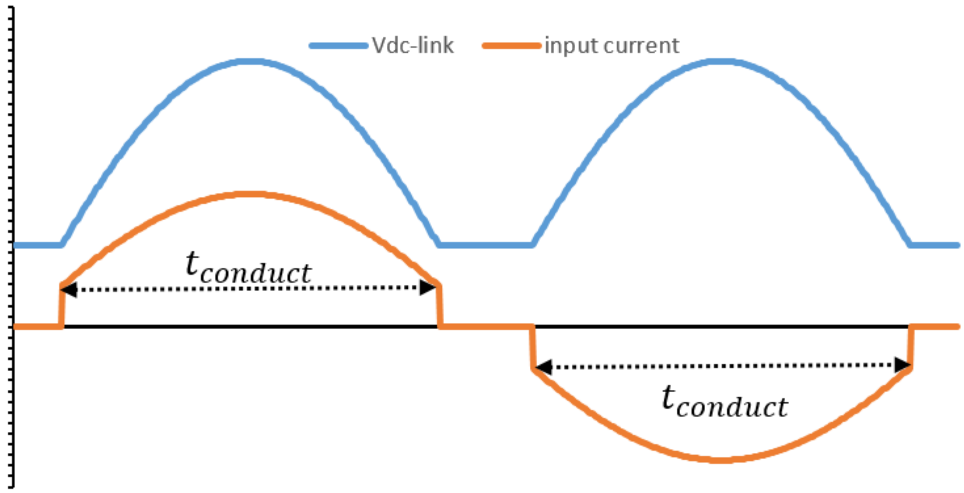

Figure 4.0.4: Input current and dc link voltage waveforms

Fluctuating Dc-link voltage causes torque fluctuations and a speed control difficulties. In order to overcome these problems various correction techniques are proposed in literature. Many researches overcome this problem by modifying the d-axis and q-axis current references which belongs to rotating reference frame.

For q axis current reference, there are there are two main approaches in the literature. The first and commonly used approach is that the shape of the q-axis current reference is modified as the square of sinusoidal wave synchronized with AC source voltage angle to maximize the input power factor. This method is used in [2, 12, 14, 15, 16, 18]. To maximize the power factor, input power signal and inverter power signal indicated in Figure 4.0.5 must be synchronized in time.

Q axis current waveform is derivatived in following equations [15]. Power consumption of capacitor can be neglected due to it has very low power relatively.

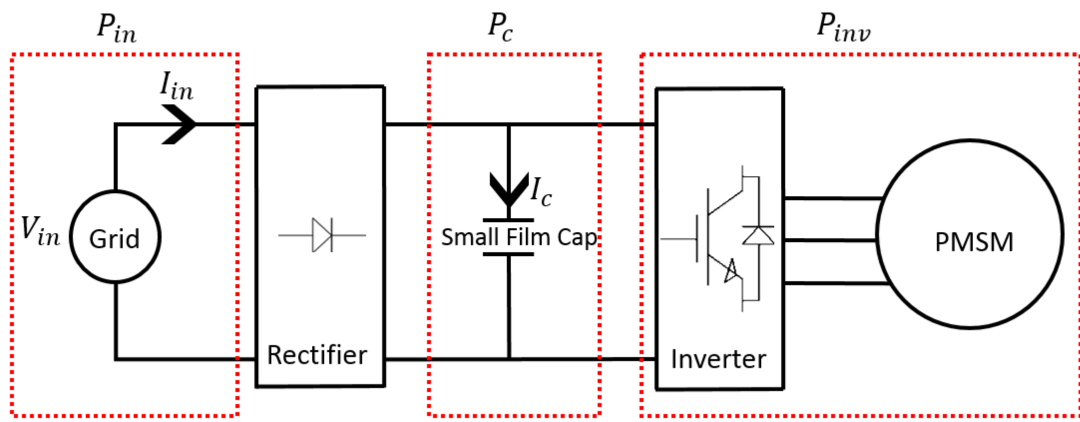

Figure 4.0.5: Input power, Dc link power and inverter power

$$P_{in} = P_c + P_{inv} \tag{4.0.2}$$

$$P_c \approx 0 \tag{4.0.3}$$

$$P_{in} \approx P_{inv} \tag{4.0.4}$$

where

$$P_{in} = V_{in} \cdot I_{in} \cdot sin^2(\vartheta \cdot t) \tag{4.0.5}$$

$$P_{inv} = 1.5 \cdot \omega \cdot [\phi + (L_d - L_q) \cdot i_d] \cdot i_q \tag{4.0.6}$$

$$V_{in} \cdot I_{in} \cdot sin^2(\vartheta \cdot t) = 1.5 \cdot \omega \cdot [\phi + (L_d - L_q) \cdot i_d] \cdot i_q \tag{4.0.7}$$

Due to $L_d = L_q$ for round rotor machines last equation can be rewritten as follow.

$$V_{in} \cdot I_{in} \cdot sin^2(\vartheta \cdot t) = 1.5 \cdot \omega \cdot \phi \cdot i_q \tag{4.0.8}$$

According to above equation, to maximize input power factor q axis current must be synchronized and proportional to square of AC source voltage angle.

$$sin^2(\vartheta \cdot t) \propto i_q \tag{4.0.9}$$

In some researches like [14, 18] q axis current is extra modified taking into account the power spent in capacitor which is shown in Figure 4.0.6

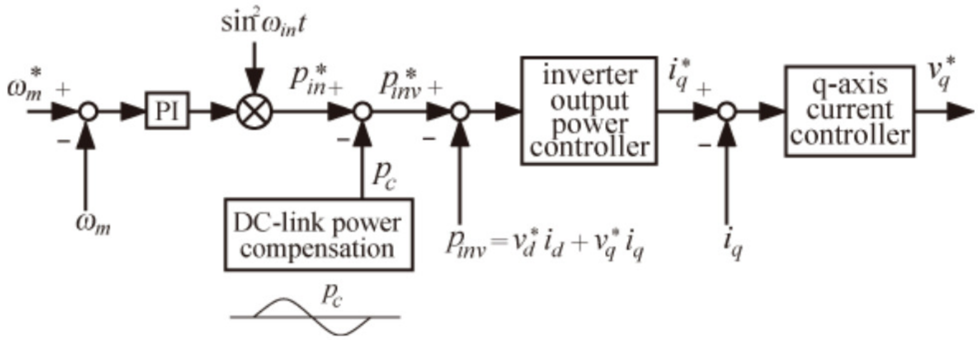

Figure 4.0.6: q axis current modulation [14]

Another approach is whereby the q-axis current reference is shaped as a trapezoidal waveform which is shown in Figure 4.0.7. However, trapezoidal q-axis current reference causes high levels of input current harmonics compared to sinusoidal q-axis current reference. Therefore, the sinusoidal current q-axis reference method is the most commonly used technique[2]

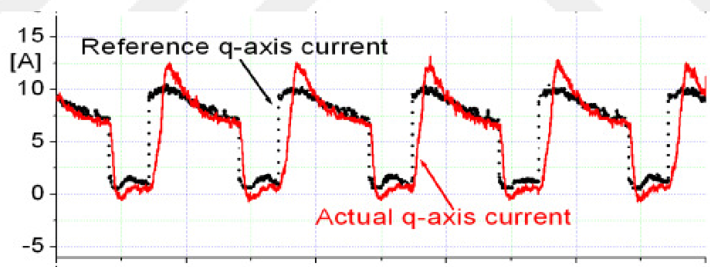

Figure 4.0.7: q axis current modulation [13]

For d axis current generation, in [12, 13, 17] current reference is calculated through a formula which is related to motor parameters. For example in [12], d axis current reference is generated by following formula.

$$i_d = -\frac{\phi}{L_d} + \frac{1}{L_d} \cdot \sqrt{(\frac{V_{om}}{\omega})^2 - (L_q \cdot i_q)^2} \tag{4.0.10}$$

where V_{om} is inverter terminal voltage. One of the biggest disadvantages is that this method is highly dependent on motor parameters.

Another method for d axis current, in studies [14], the d-axis current command is expressed as a constant value corresponding to the speed and the load torque.
In another study [2], d-axis current reference changes very slowly according to average voltage constraint concept. The "average voltage" is the mean value of the fluctuating dc-link voltage during a half period of the source voltage represented on the d, q-axis current plane. The voltage is used as the constraint applied to the flux-weakening controller, which generates the d-axis current reference. d and q axis current modulation using in [2] is shown in Figure 4.0.8.

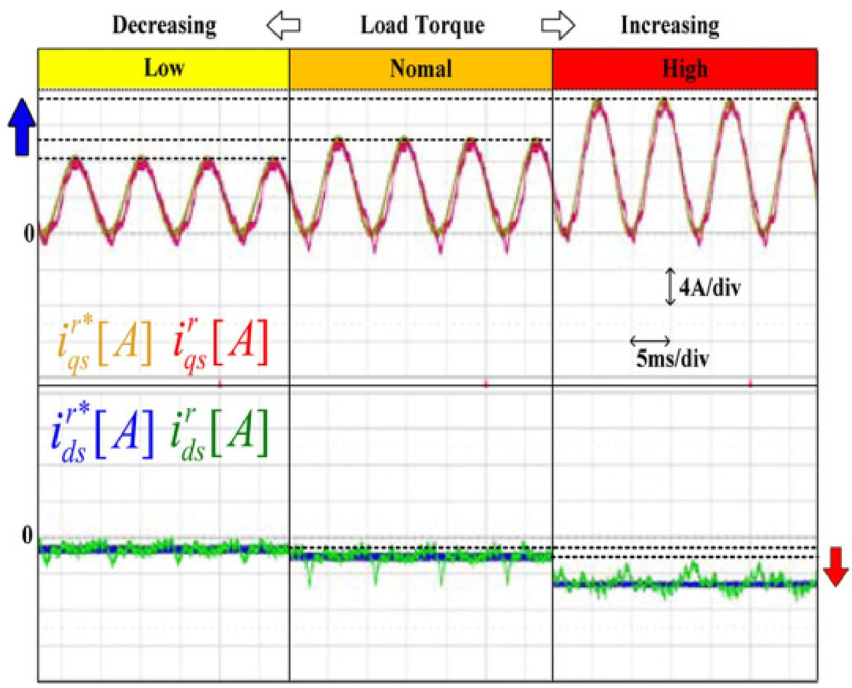

Figure 4.0.8: d and q axis current modulation using in [2]

In another study [16], the d-axis current reference is set at a negative constant value by trial-and-error after changing operating point so that the system obtains a high power factor which is shown in Figure 4.0.9

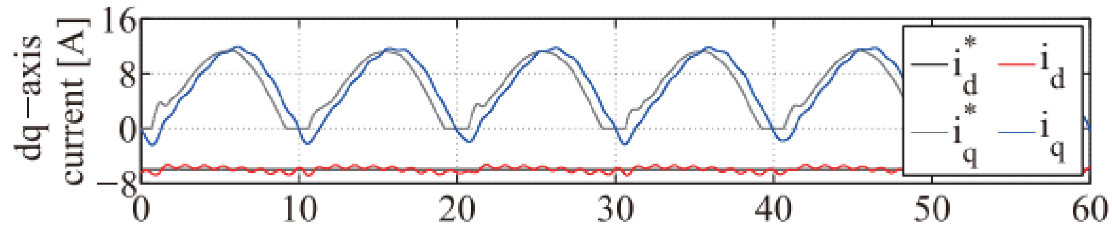

Figure 4.0.9: d and q axis current modulation using in [16]

In study [15], a slightly different method is proposed which is shown in Figure 4.0.10, but, d-axis current reference waveform ends up to be too sharp. In order to achieve control loop with such a sharp reference, a PR controller is used as a current control which is difficult to implement in comparison to a standard PI controller.

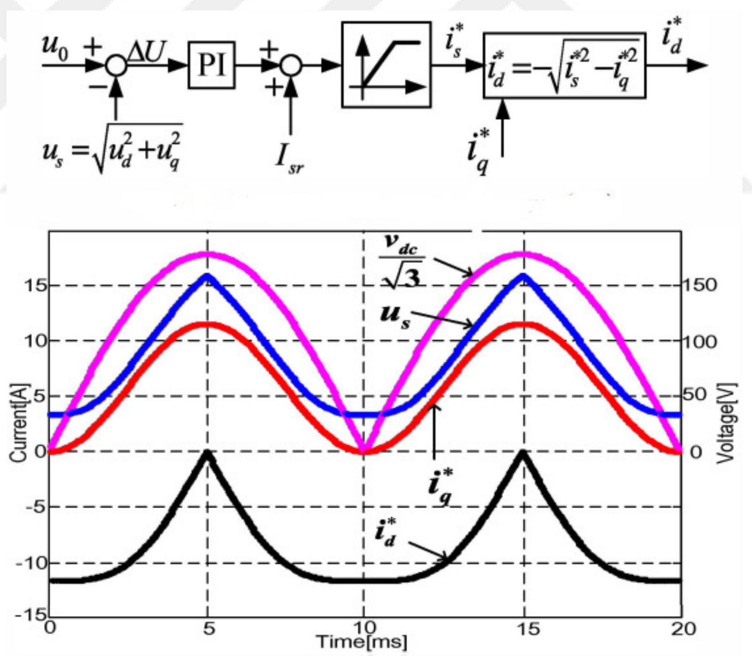

Figure 4.0.10: d and q axis current modulation using in [15]

CHAPTER V

PROPOSED METHOD FOR SPEED CONTROL OF PMSM WITHOUT ELECTROLYTIC CAPACITOR

The method investigated in this control system proposal is shown in Fig 5.0.3. Q-axis current reference is modified as the square of sinusoidal wave synchronized with AC source voltage angle just like most studies in the literature. Unlike other methods in literature however, the d-axis current reference is modified as the square of cosinusoidal wave synchronized again with ac source voltage angle. The basic motivation behind the proposed method is to apply d current only when needed or in other words, always trying to keep the motor in motor region instead of regenerative region. As mentioned before, dc-link voltage fluctuates at twice the frequency of the grid due to rather small capacitor allocation. At the peak of the dc-link voltage, it can be considered as a large capacity system. So, there is no need for d-axis current around at peak value of dc-link voltage under nominal speed. Because applicable source voltage is greater than motor terminal voltage. So there is no need to flux weakening operation here. Similarly, there is much more need to d-axis current around lower value of dc-link voltage. Because applicable source voltage is too lower than motor terminal voltage. So there is much more need to flux weakening operation here. As a result, d-axis current waveform should be follow a square of cosinusoidal which is synchronized with ac source voltage angle. This method is illustrated in Fig 5.0.1 Amplitude of d-axis current is adjusted with voltage margin PI controller. Voltage margin means difference between maximum applicable source voltage and motor terminal voltage. Maximum applicable source voltage, motor terminal voltage and voltage margin can be calculated as follows. Also voltage margin PI controller

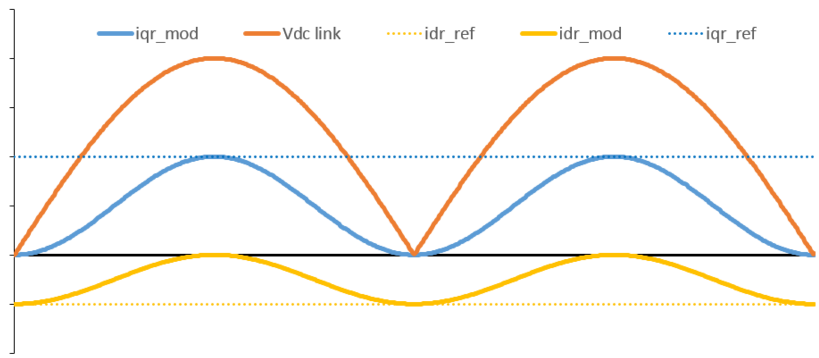

Figure 5.0.1: Proposed d axis and q axis current waveform

operates as shown Figure 5.0.2

$$V_{applicable} = V_{bus} \cdot \frac{1}{\sqrt{3}} \tag{5.0.1}$$

$$V_{motorterminal} = \sqrt{V_\alpha^2 + V_\beta^2} \tag{5.0.2}$$

$$V_{margin} = V_{applicable} - V_{motorterminal} \tag{5.0.3}$$

If voltage margin reference value is too high, unnecessary extra d current is applied

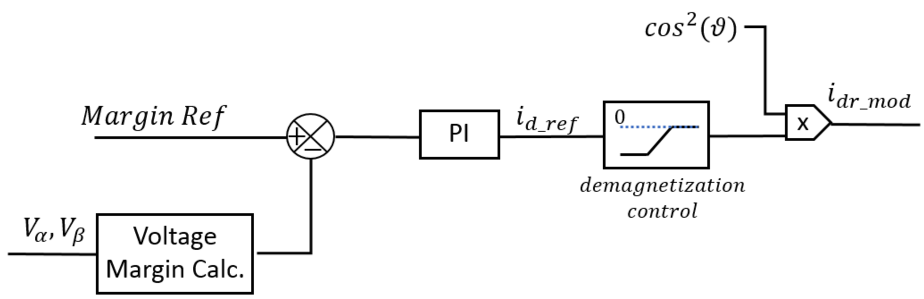

Figure 5.0.2: d axis current reference generation with voltage margin PI

and it causes the power factor to drop. Similarly, if voltage margin reference value is too low, there will be disruptions in torque control since enough d current cannot be applied. Therefore, the voltage margin reference value is obtained with fine tuning at working conditions with load. In order not to disturb sinusoidal waveform of idr_{mod} and iqr_{mod} , idr_{ref} and iqr_{ref} are determined at every zero crossing event.

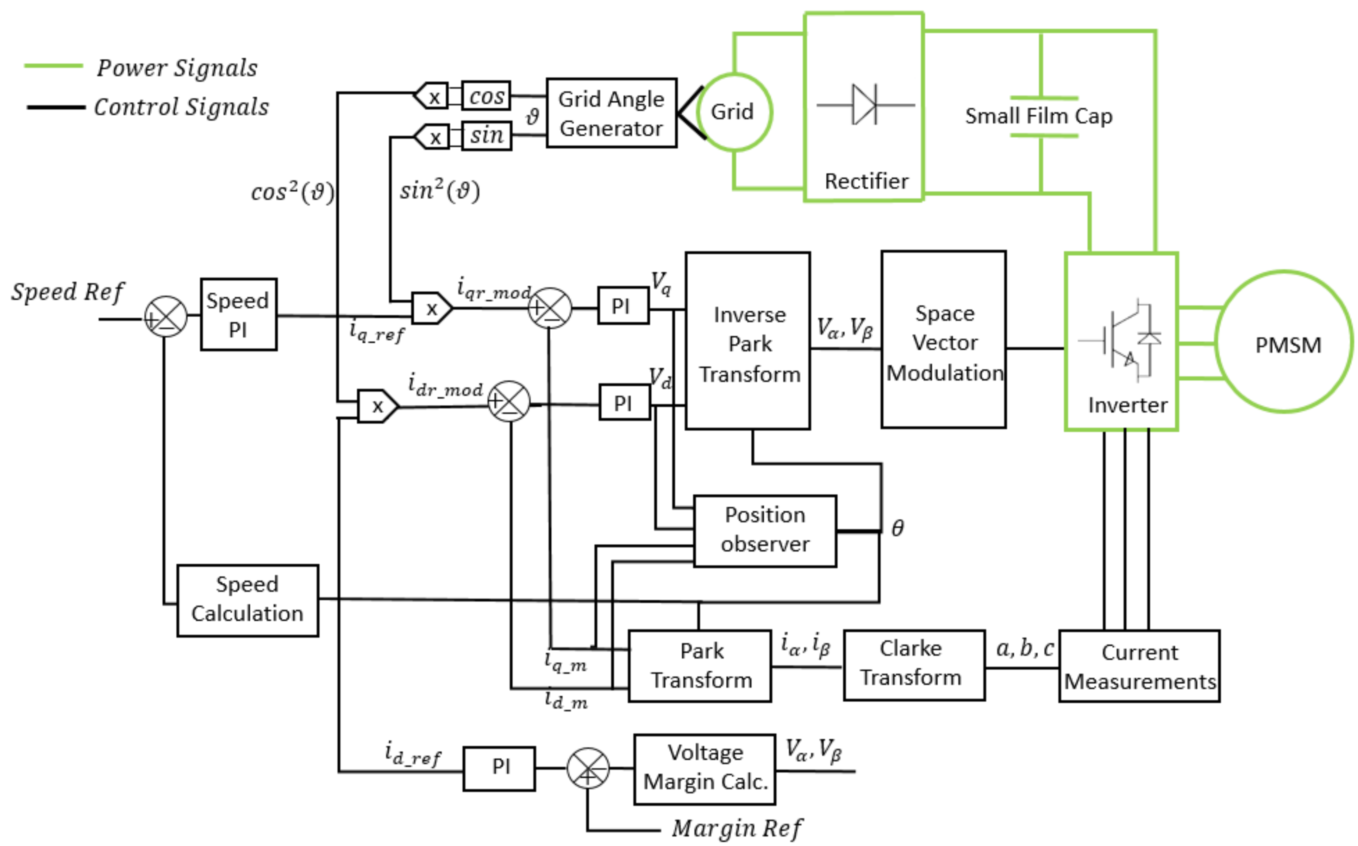

Figure 5.0.3: Overall proposed modulated field oriented control diagram without electrolytic capacitor and position sensor.

5.1 Simulation Results

In order to verify the validity of proposed technique, as well the performance and stability improvements that can be attained, a detailed computer simulation has been performed by MATLAB/SIMULINK. The motor parameters shown in Table-1 are used in the simulations. The same design parameters were employed in experimental setup, too. Also, $10uF$ film capacitor is used as a dc-link capacitor and no additional inductor is used. Most commonly used d-axis method was also simulated to compare the performance with respect to the performance of the proposed technique.

Table 1: Motor parameters

Pole	3 Phase 6 Pole
Rated Output	790 Watts
Rated Speed	3600 rpm
Winding Resistances	2.790 ± 7% Ohms
Inductance (Ld)	$6.9mH$
Inductance (Lq)	$10.8mH$
Back EMF	42.5 Vrms / krpm (Line-to-Line) at 25C

Figure 5.1.1 and Figure 5.1.2 shows the speed performance at nominal speed and rated torque with traditional method and this work, respectively. In proposed method, speed oscillation levels are almost same but slightly higher than traditional one. Figure 5.1.3 and Figure 5.1.4 shows grid voltage (230V AC 50Hz) and input current waveform at nominal speed and rated torque with traditional method and proposed technique, respectively. Also, Figure 5.1.5and Figure 5.1.6 shows modified d-axis currents and q-axis currents waveforms at nominal speed and rated torque with respect to both cases. In simulation results, proposed method power factor is 0.97 while traditional method power factor is 0.95.

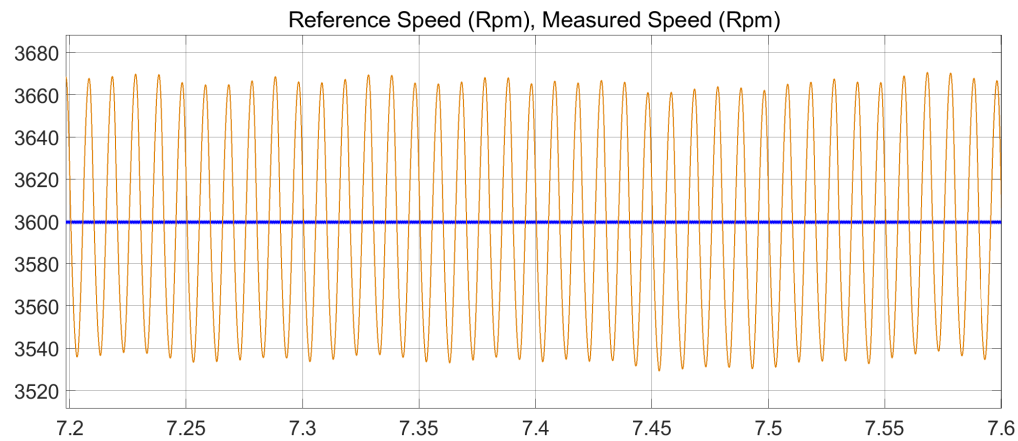

Figure 5.1.1: Speed performance at nominal speed and rated torque with traditional method

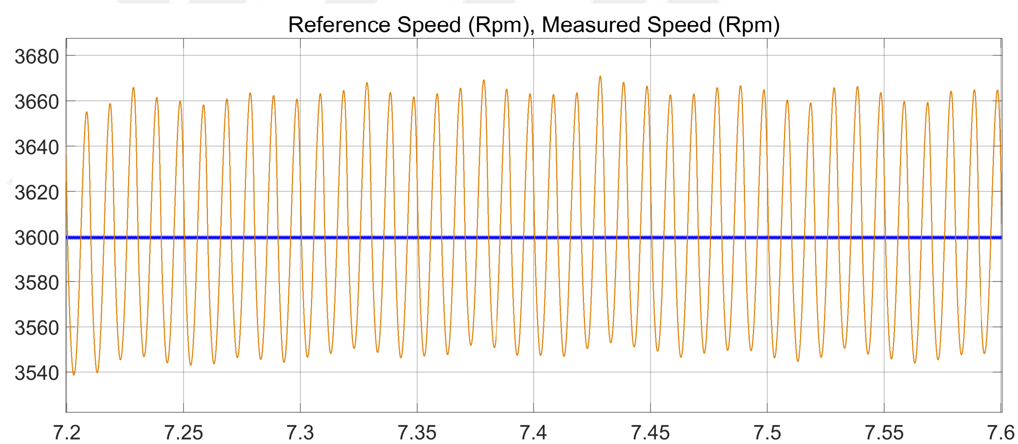

Figure 5.1.2: Speed performance at nominal speed and rated torque with proposed method

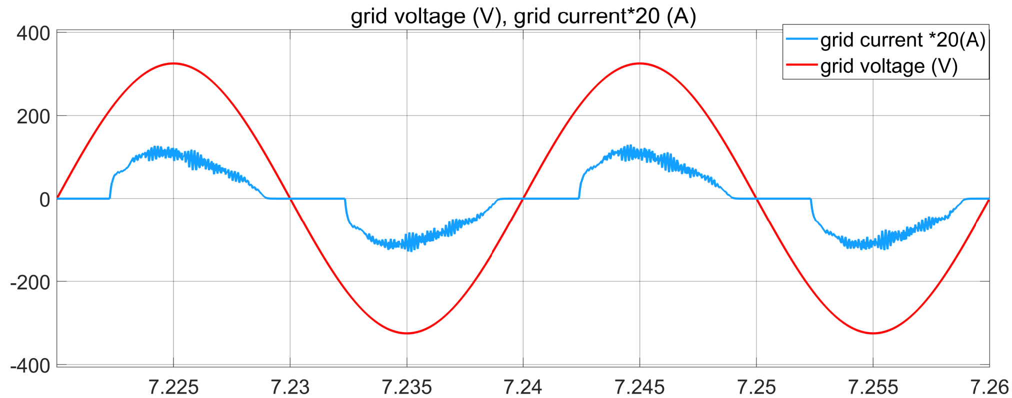

Figure 5.1.3: Grid voltage and input current waveform with 0.95 power factor at nominal speed and rated torque with traditional method

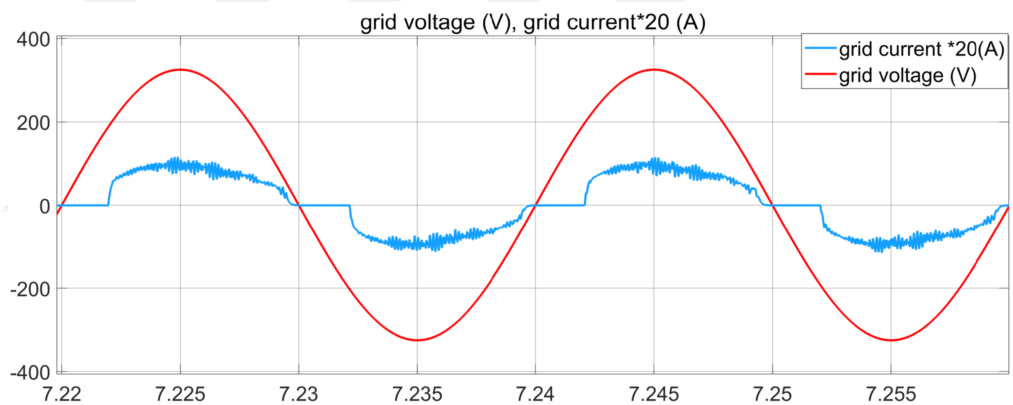

Figure 5.1.4: Grid voltage and input current waveform with 0.97 power factor at nominal speed and rated torque with proposed method.

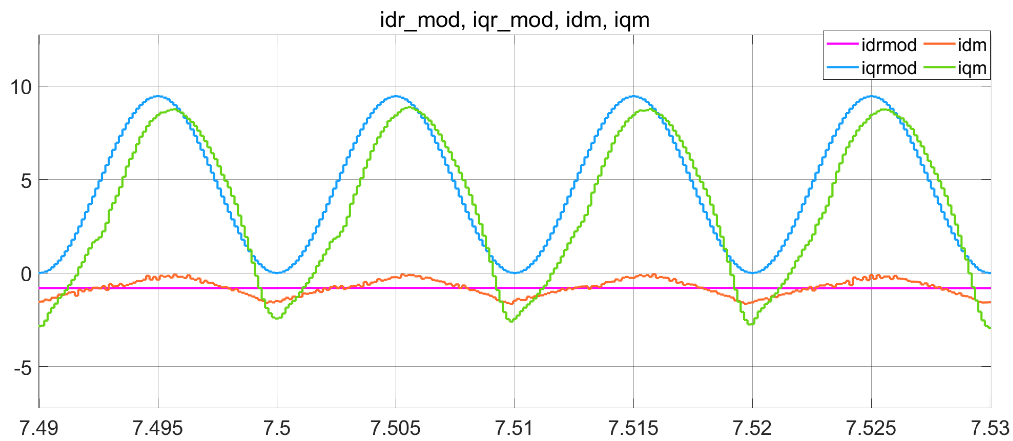

Figure 5.1.5: Modified d-axis and q-axis currents at nominal speed and rated torque with traditional method

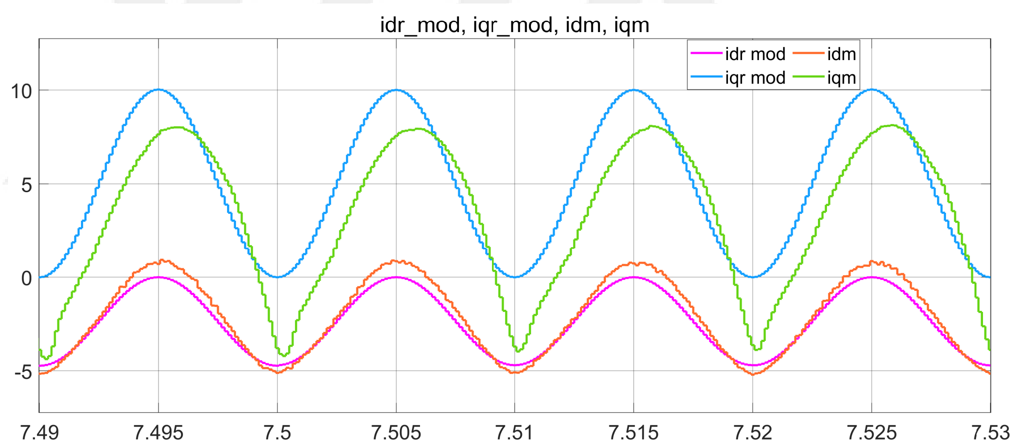

Figure 5.1.6: Modified d-axis and q-axis currents at nominal speed and rated torque with proposed method

5.2 *Experimental Results*

The standard techniques and this particular method were compared in terms of power factor and input current harmonic performance during experimental work. For input current harmonics, IEC6 1000-3-2 Class A regulation defines the harmonics limit which is very important criteria especially for air conditioning applications. Hence, the experimental work is done at an air conditioner setup which is shown Fig. 11. In the experiment, the supply voltage is 230Vac and 50 Hz. The inverter board in the figure is designed with electrolytic capacitor. The card was prepared for testing by removing the electrolytic capacitors and installing two $5uF$ film capacitors from the outside.

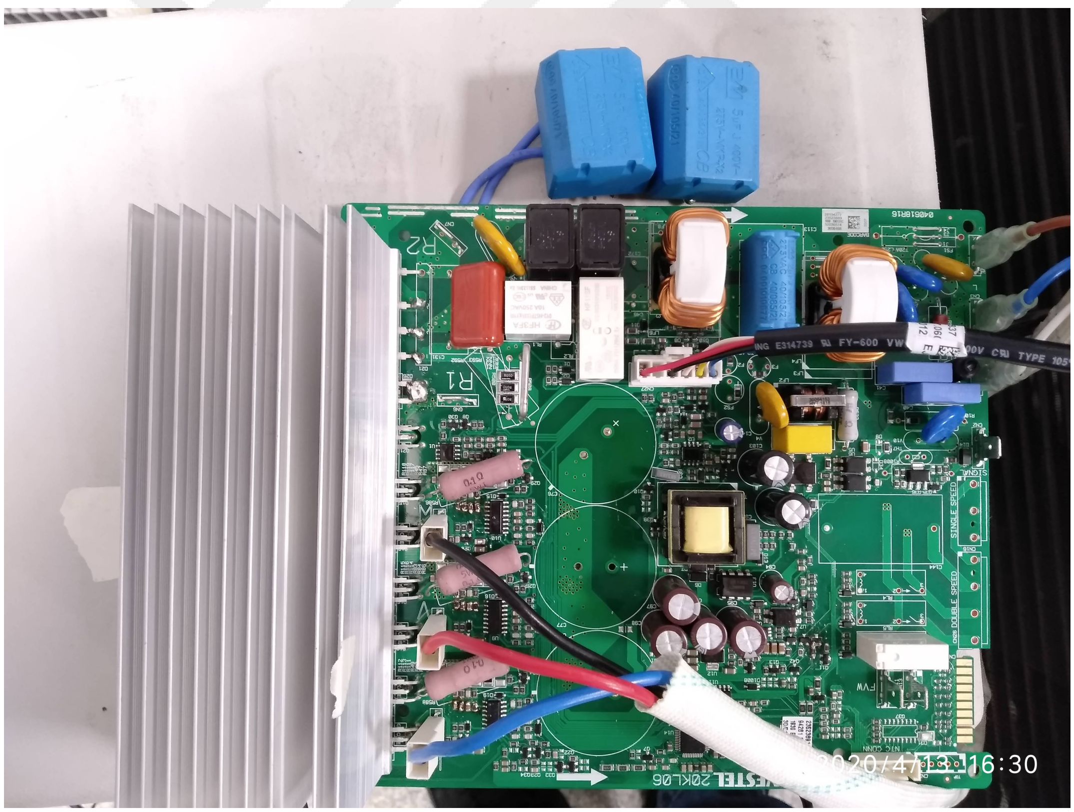

Figure 5.2.1: Inverter board with 10uF film capacitor

Figure 5.2.2: Air conditioner setup including inverter board with 10uF film capacitor

Figure 5.2.3 and Figure 5.2.4 show grid voltage and input current waveform at nominal speed and rated torque with traditional method and proposed method respectively. In experimental results, in the work proposed power factor is 0.924 while traditional method power factor is 0.96.

Figure 5.2.5 and Figure 5.2.6 shows input current harmonic results with traditional method and proposed method respectively in terms of IEC6 1000-3-2 Class A regulation. According to test results, the study has provided better input current harmonic performance.

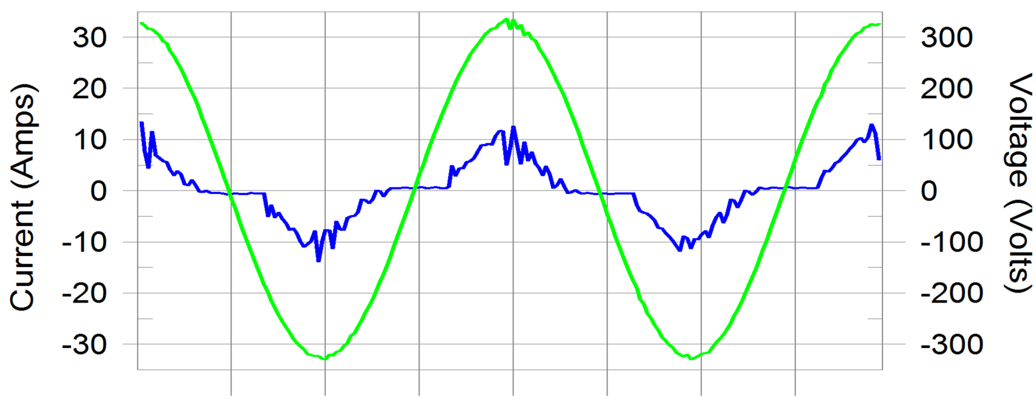

Figure 5.2.3: Supply voltage and input current waveform at nominal speed with power factor 0.924 with traditional method

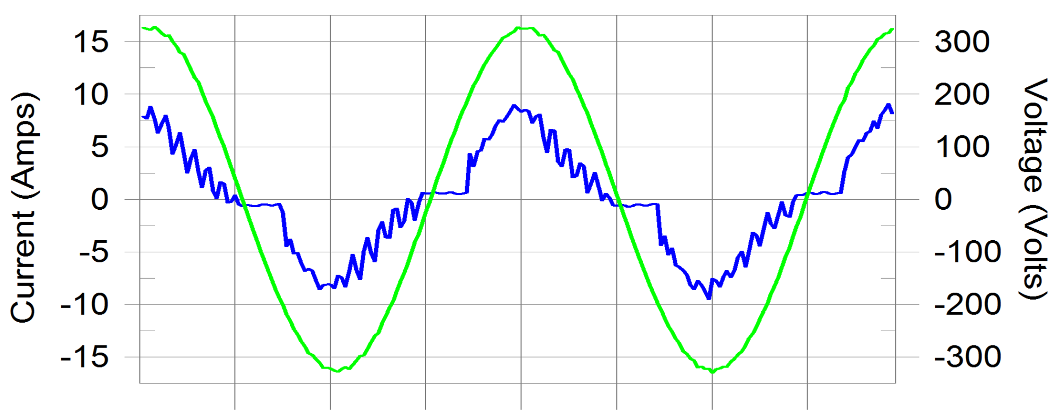

Figure 5.2.4: Supply voltage and input current waveform at nominal speed with power factor 0.96 with proposed method

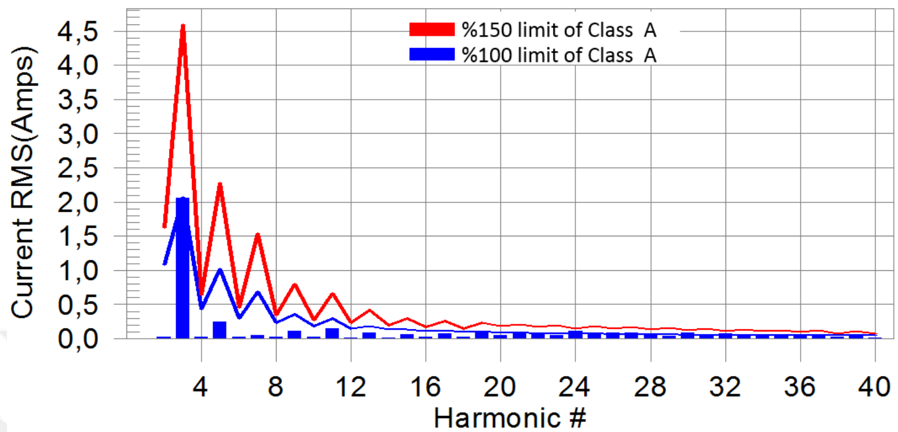

Figure 5.2.5: Supply voltage and input current waveform at nominal speed with power factor 0.924 with traditional method

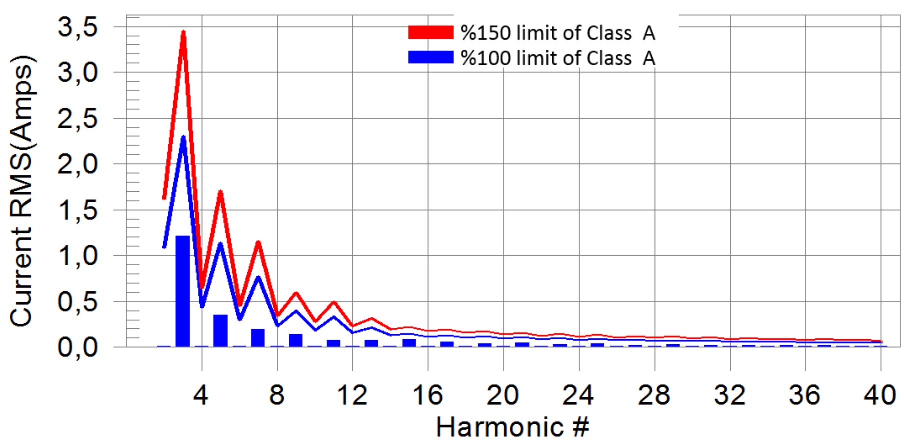

Figure 5.2.6: Supply voltage and input current waveform at nominal speed with power factor 0.924 with traditional method

CHAPTER VI

CONCLUSION

This thesis proposes a new flux weakening strategy by a different d-axis current waveform injection than the ones introduced in prior literature. The method has provided a better input current harmonics performance and hence, provides high power factor compared to traditional methods at nominal speed conditions. For future work, above the nominal speed levels, this method must be modified by adding dc offset to cosinusoidal d-axis current waveform. Performance improvements and validity of the proposed method is verified experimentally by comparison with respect to the traditional harmonic cancellation methods.

Bibliography

[1] Kyu-Dong Kim, Young-Ho Kim, Jun-Gu Kim, Yong-Chae Jung, and Chung-Yuen Won, "A new active power decoupling technique for three-port flyback inverter," *Proceedings of The 7th International Power Electronics and Motion Control Conference*, vol. 2, no. 2, pp. 1159–1163, 2012.

[2] H. Jung, S. Chee, S. Sul, Y. Park, H. Park, and W. Kim, "Control of three-phase inverter for ac motor drive with small dc-link capacitor fed by single-phase ac source," *IEEE Transactions on Industry Applications*, vol. 50, no. 2, pp. 1074–1081, 2014.

[3] J. S. D. U. A. E. Fitzgerald, Charles Kingsley, *ELECTRIC MACHINERY 6th Ed.* McGraw-Hill, 2003.

[4] E. Lomonova, J. Paulides, E. Kazmin, and L. Encica, "In-wheel pm motor: Compromise between high power density and extended speed capability," *COMPEL - The international journal for computation and mathematics in electrical and electronic engineering*, vol. 30, 01 2011.

[5] H. Taha and I. Alnaab, "Designs of pmsms with inner and outer rotors for electric bicycle applications," *Kurdistan Journal of Applied Research*, vol. 4, pp. 20–25, 06 2019.

[6] F. B. A. Oussama BOUAZIZ, Imen JAAFAR, "Performance analysis of radial and axial flux pmsm based on 3d fem modeling," *Turkish Journal of Electrical Engineering and Computer Sciences*, p. 1587 – 1598, 2018.

[7] C. Busca, "Open loop low speed control for pmsm in high dynamic applications," Tech. Rep. STAN-CS-83-980, Departament of Energy Tehnology, Aalborg University, 2010.

[8] D. Ocen, "Direct torque control of a permanent magnet synchronous motor," Tech. Rep. IR-RT-EX-0509, Motion Control and Industrial Applicaitons, Universitat Politecnica de Catalunya, Stockholm, Sweden, 2005.

[9] M. F. Marek Stulrajter, Val´eria Hrabovcova, "Permanent magnets synchronous motor control theory," *Journal of ELECTRICAL ENGINEERING*, vol. 58, p. 79 – 84, Mar 2007.

[10] R. R. Sandeep J, Ashok S, "Carrier based space vector modulation for matrix converters," *1st IEEE International Conference on Power Electronics. Intelligent Control and Energy Systems*, 2016.

[11] R. R. Sandeep J, Ashok S, "Carrier based space vector modulation for matrix converters," *1st IEEE International Conference on Power Electronics. Intelligent Control and Energy Systems*, 2016.

[12] I. Takahashi and H. Haga, "Power factor improvement of single-phase diode rectifier by fast field-weakening of inverter driven ipm motor," *4th IEEE International Conference on Power Electronics and Drive Systems. IEEE PEDS 2001 - Indonesia. Proceedings (Cat. No.01TH8594)*, vol. 1, pp. 241–246 vol.1, 2001.

[13] H. Lamsahel and P. Mutschler, "Permanent magnet drives with reduced dc-link capacitor for home appliances," *2009 35th Annual Conference of IEEE Industrial Electronics*, pp. 725–730, 2009.

[14] K. Inazuma, K. Ohishi, and H. Haga, "High-power-factor control for inverter output power of ipm motor driven by inverter system without electrolytic capacitor," in *2011 IEEE International Symposium on Industrial Electronics*, pp. 619–624, 2011.

[15] Hui Luo, Genping Wu, and Quan Yin, "Proportional-resonant control of a single-phase to three-phase converter without electrolytic capacitor," in *2015 Chinese Automation Congress (CAC)*, pp. 1798–1803, 2015.

[16] K. Abe, H. Haga, K. Ohishi, and Y. Yokokura, "Fine current harmonics reduction method for electrolytic capacitor-less and inductor-less inverter based on motor torque control and fast voltage feedforward control for ipmsm," *IEEE Transactions on Industrial Electronics*, vol. 64, no. 2, pp. 1071–1080, 2017.

[17] A. Yoo, S. Sul, H. Kim, and K. Kim, "Flux-weakening strategy of an induction machine driven by an electrolytic-capacitor-less inverter," *IEEE Transactions on Industry Applications*, vol. 47, no. 3, pp. 1328–1336, 2011.

[18] K. Abe, K. Ohishi, and H. Haga, "Input current harmonics reduction control for electrolytic capacitor less inverter based ipmsm drive system," in *2014 International Power Electronics Conference (IPEC-Hiroshima 2014 - ECCE ASIA)*, pp. 3153–3158, 2014.

VITA

Seyit YILDIRIM is received the B.Sc. degree from Electrical and Electronics Engineering Department of Ege University, Izmir, Turkey, in 2017. He has been working at VESTEL Electronics as Motor Control Software Engineer since 2017. His research interests are motor control systems, software design and power electronics.